Brain Stimulation 15 (2022) 260–269

Contents lists available at ScienceDirect

Brain Stimulation

journal homepage: http://www.journals.elsevier.com/brain-stimulation

Auricular transcutaneous vagus nerve stimulation modulates the heart-evoked potential

Tasha Poppa [a, b, *], Lars Benschop [a], Paula Horczak [a], Marie-Anne Vanderhasselt [a], Evelien Carrette [c], Antoine Bechara [b], Chris Baeken [a, d, e], Kristl Vonck [c]

[a] Ghent Experimental Psychiatry Lab, Psychiatry and Medical Psychology, Department of Head and Skin, Ghent University Hospital, Belgium
[b] Department of Psychology, University of Southern California, Los Angeles, CA, USA
[c] 4Brain, Neurology, Department of Head and Skin, Ghent University Hospital, Belgium
[d] Department of Psychiatry, Brussels University Hospital, Belgium
[e] Department of Electrical Engineering, Eindhoven University of Technology, the Netherlands

ARTICLE INFO

Article history:
Received 20 August 2021
Received in revised form
28 November 2021
Accepted 15 December 2021
Available online 18 December 2021

Keywords:
Transcutaneous
Auricular
Vagus nerve stimulation
Insula
Interoception
Heart-evoked potential
Electroencephalography
Source-localization
Central autonomic network

ABSTRACT

Background: There is active interest in biomarker discovery for transcutaneous auricular vagus nerve stimulation (taVNS). However, greater understanding of the neurobiological mechanisms is needed to identify candidate markers. Accumulating evidence suggests that taVNS influences activity in solitary and parabrachial nuclei, the primary brainstem relays for the transmission of visceral sensory afferents to the insula. The insula mediates interoception, which concerns the representation and regulation of homeostatic bodily states. Consequently, interoceptive pathways may be relevant to taVNS mechanisms of action.

Hypotheses: We hypothesized that taVNS would modulate an EEG-derived marker of interoceptive processing known as the heart-evoked potential (HEP). We also hypothesized that taVNS-induced HEP effects would be localizable to the insula.

Methods: Using a within-subject, sham-controlled design, we recorded EEG and ECG concurrent to taVNS in 43 healthy adults. Using ECG and EEG data, we extracted HEPs. Estimation of the cortical sources of the taVNS-dependent HEP responses observed at the scalp were computed using the Boundary Element Method and weighted Minimum Norm Estimation. Statistics were calculated using cluster-based permutation methods.

Results: taVNS altered HEP amplitudes at frontocentral and centroparietal electrode sites at various latencies. The taVNS-dependent HEP effect was localized to the insula, operculum, somatosensory cortex, and orbital and ventromedial prefrontal regions.

Conclusion: The results support the hypothesis that taVNS can access the insula as well as functionally and anatomically connected brain regions. HEPs may serve as an objective, non-invasive outcome parameter for the cortical effects of taVNS.

There is active interest in biomarker discovery for transcutaneous auricular vagus nerve stimulation (taVNS) [1]. However, the mechanisms underpinning the neurobiological effects of taVNS remain unclear, thereby hampering the identification of markers that either directly or indirectly reflect the relevant pathophysiological systems in brain disorders indicated for taVNS. We propose that activation of the interoceptive pathways to the insula as a candidate systems-level mechanism of taVNS. Following this perspective, we conducted a proof-of-concept investigation to determine whether the heart-evoked potential (HEP), an EEG-derived marker of cardiac interoceptive processing, could be modified by taVNS.

Interoception describes the representation and integration of homeostatic sensory signals from the viscera, muscles, and skin

Abbreviations: AVBN, Auricular branch of the vagus nerve; GAN, Greater auricular nerve; HEP, Heart evoked potential; NST, Nucleus of the solitary tract; taVNS, transcutaneous auricular vagus nerve stimulation; VNS, Vagus nerve stimulation.

* Corresponding author. Ghent University Hospital, 1K12F, Corneel Heymanslaan 10, 9000, Ghent, Belgium.
E-mail address: natalie.poppa@ugent.be (T. Poppa).

https://doi.org/10.1016/j.brs.2021.12.004

that ascend to the brain via spino-cranial lamina I (L1) afferents and vagal, facial, and glossopharyngeal nerve afferents to parabrachial nucleus (PBN) and the nucleus of the solitary tract (NST) [2–4]. The NST and PBN in turn, relay interoceptive afferents to the dorsal mid-posterior insula via the basal and posterior sectors of the ventro-medial thalamic nucleus [2].

While functionally and anatomically complex, the insula can be broadly parcellated along granular, dysgranular, and agranular cytoarchitectonic boundaries [5]. A current model of the primate insula proposes that the posterior sector of the dorsal granular insula receives spinal LI projections whereas solitary tract projections are located more anteriorly, reflecting a spino-cranially organized functional topography [6]. The intermediate dysgranular region of the insula is also proposed to integrate primary interoceptive representations with polymodal cortical and subcortical inputs, which are then funneled to the anterior agranular sector, a subregion that is functionally and anatomically interconnected with the anterior cingulate cortex (ACC) and orbitofrontal cortex (OFC) [6]. The anterior insula, OFC, and ACC, in turn, project to limbic and brainstem pre-autonomic and neuroendocrine effector nuclei, including the amygdala, hypothalamus, PBN, and periaqueductal gray (PAG) [5–7]. In sum, the insula is positioned as a cortical hub in a neurovisceral hierarchy that interfaces interoceptive sensory information with the brain's visceromotor functions— which is to say that the insula contributes to how the brain dynamically regulates autonomic, hormonal, and metabolic outputs to meet the homeostatic demands of the body [5].

There is a role for the interoceptive system and its visceromotor complement neuropsychiatric disorders indicated for taVNS. Mood and anxiety disorders present with significant somatic disturbances, such as altered immune function [8–10], reduced parasympathetically-mediated heart rate variability [11,12], hypothalamic-pituitary-adrenal (HPA)-axis abnormalities [13], pain [14,15], altered appetite and body mass [16,17], and increased risk of cardiovascular disease [18–20]. Atypical structure and function of the insula, ACC, and OFC are also believed to contribute to the pathophysiology of mood and anxiety disorders [21–27]. Moreover, reduced gray matter volume in the bilateral insula and ACC are common to multiple neuropsychiatric disorders according to a large-scale meta-analysis of over 15,000 patients [28], suggesting that interoceptive-visceromotor dysregulation may be a transdiagnostic feature.

In turn, stimulation of viscerosensory pathways, directly via invasive and non-invasive vagus nerve stimulation (VNS) or indirectly via cardiorespiratory exercises such as heart rate variability (HRV) biofeedback, has been found to reduce mood and anxiety symptoms and attendant autonomic and neuroendocrine dysfunctions [29–34]. Hence, functional alterations in thalamocortical interoceptive pathways may be one systems-level mechanism by which taVNS could reduce symptom burdens in multiple disorders. Functional magnetic resonance imaging (fMRI) investigations support the idea that taVNS alters BOLD activity within interoceptive pathways. At the level of the brainstem, responses within the PBN and NST have been observed [35–39]. Although the auricular branch of the vagus nerve (AVBN) is conventionally described as belonging to the spinal trigeminal system [40], tract-tracing experiments in animals have identified projections from the AVBN to the NST [41]. Additional taVNS studies highlight increased neural activity or altered BOLD responses within the locus coeruleus [36,37,42–45], which is a major target of adrenergic influence that also has bidirectional communication with the NST [46]. Above the brainstem, taVNS elicits BOLD responses within the insula, ACC, OFC, hypothalamus, thalamus, and amygdala [36,40,44,47–49].

If taVNS modulates brain function via L1 and NST projections that ascend to the insula, neurophysiological indices of interoceptive processing should be sensitive to taVNS. The heart-evoked potential (HEP) is one such measure believed to reflect neural processing of cardiac dynamics that are transduced by vagal, glossopharyngeal, and spinal L1 afferents that are integrated within the insula and operculum [50]. The sensitivity of HEPs to taVNS remains to be established.

The HEP is an endogenous cortical evoked potential that is time-locked to the peak of the ECG R-wave [51]. According to meta-analysis, the HEP is characterized by voltage deflections at frontal, central, and frontocentral electrode locations at latencies around 200–500 ms [52]. HEPs are responsive to interoceptive attention tasks [53,54], emotional stimuli [55,56], and have been found to reflect clinical status in studies of depression [57], anxiety [58], hypertension [59], ventricular cardiac dysfunction [60] and diabetic autonomic neuropathy [61]. Human intracranial EEG and ECoG studies have furthermore confirmed that HEPs can be recorded from interoceptive, visceromotor, and somatosensory brain regions [50,62–64].

The present study evaluated whether taVNS acutely modifies HEPs in healthy adults in a randomized, sham-controlled, within-subjects EEG study. Based on fMRI evidence suggesting that taVNS activates interoceptive-autonomic networks, and given that the insula represents the cortical hub of interoceptive processing, we hypothesized that taVNS would alter HEPs. We further hypothesized that current source estimation of the HEP difference (i.e., active taVNS – sham) would confirm the involvement of the insula.

1. Methods and materials

1.1. Participants

Participants were recruited from university communities and the greater community in Flanders, Belgium. Participants were eligible if they were 18–45 years old, right-handed, free of medical and psychiatric conditions, non-user of nicotine products, free of extensive ear piercings, and not taking medication that could affect the autonomic nervous system. Forty-eight participants were recruited, but three were later dropped due to discovery of left-handedness, psychiatric illness, and ECG abnormalities. Hence, 45 subjects (18M:27F) participated (Age: M = 23.1, SD = 5.01). However, 43 were included in final analyses as two participants did not return for the second EEG session. Data were collected from September 2018 – June 2019. The study was approved by the University of Southern California IRB and the Ghent University Hospital Medical Ethics Committee.

2. Study design

Subjects participated in a single-blind, within-subjects experiment during which sham or taVNS was applied on separate days. Sessions were spaced at least 24 h but less than one week apart. The order of conditions for a given session and participant was randomized using a simple computer-generated sequence. Each experimental session involved cardiovascular and EEG recordings, and self-report questionnaires. During a session, participants sat upright in a reclining chair with their legs comfortably elevated. Participants were instructed to keep their eyes “half” open during EEG recording, such that they found a point on which to fix their gaze at a level low enough to reduce tension in the facial muscles and prevent eye strain. This instruction was intended to reduce the presence of muscle artifacts in the EEG data. EEG and cardiovascular recordings were obtained for a baseline period (10 min), after which participants completed reported their present level of

anxiety using the state subscale of the State-Trait Anxiety Inventory (STAI) [65]. Participants were then fit with the taVNS device, whereafter an individualized current intensity was established (see **taVNS procedure**). EEG and cardiovascular recordings were obtained concurrent to stimulation (15 min), after which participants completed the STAI a second time. Next, participants provided ratings of stimulation-induced pain and the intensity of perceived pricking, pressing and dull sensations (scale: 0–10). The sensation questions were intended to elucidate whether there was indication of Aδ or even C-fiber activation after the 15-min. stimulation period [66]. The device was turned off and data were recorded during a 10 min recovery period after which participants completed the STAI for a third time.

2.1. taVNS procedure

Details of the procedure are described in accordance with recommendations outlined in Farmer et al. (2020) [67]. Participants received taVNS using the NEMOS® device (Cerbomed, Erlangen, Germany), which is CE-marked for treatment-resistant epilepsy (Cerbomed's related VITOS® device is CE-marked for pain and depression). The device has an adjustable earpiece containing titanium anodal and cathodal ball-point electrodes connected to a stimulator. The device was used to provide transcutaneous electrical stimulation of the left AVBN via the cymba conchae (taVNS) as well as control stimulation of the left greater auricular nerve (GAN) via the earlobe (sham). Stimulation parameters consisted of 0.25 ms-duration monophasic square wave pulses at 25 Hz with a customized rapid duty cycle of 7 s on and 18 s off [68]. The stimulation site was first exfoliated with abrasive gel and cleaned with alcohol to minimize impedance. Impedance was measured automatically by the device and insufficient electrode contact with the skin evoked a beep.

To set individual current intensities and match the quality of sensations across the taVNS and sham, a method of limits was used to determine the level that evoked a clear tingling sensation without pain or significant unpleasantness. Tingling sensations reflect the recruitment of low-threshold, thickly myelinated Aβ fibers [69]. The intensity was slowly increased from 0.1 mA in increments of 0.1 mA until the participant first detected a tingling sensation, recorded as the perceptual threshold. The intensity was increased in 0.1 mA increments until the sensation was reported to be unpleasant or pricking (exciting Aδ fibers [66]). This procedure was repeated three times. The average of the detection and pain thresholds was set as the stimulation intensity. Participants were informed that the current levels should be tolerable throughout the 15-min of stimulation, and that they could ask for the current intensity to be reduced if they developed sensitivity.

2.2. Data acquisition

A Micromed System Plus (Micromed, Mogliano, Italy) with Ag/AgCl electrodes were used to record EEG at 60 standard locations according to the international 10-10 system using a 64 channel WaveGuard cap (ANT Neuro, Netherlands). Cz was used for referencing during online acquisition, and AFz was used as the ground. Vertical and horizontal electrooculogram (EOG), respiration (RESP), electrocardiogram (ECG) and pulse oximetry (PO) were recorded using bipolar channels. O1, O2, PO7, and PO8 were omitted from the EEG montage to make recording channels available for physiological data. For ECG, one electrode was placed below the right midclavicle and the other was placed on a lower left rib, producing a high-amplitude R-wave to facilitate automatic peak detection. EEG, EOG, RESP, ECG, and PO were digitized online using a sampling rate of 1024 Hz and online high-pass filter of 0.008 Hz. Electrode impedances for the EEG channels were stabilized below 5 kΩ before recordings commenced. RESP and PO data were not considered for the present report.

2.3. Statistical modeling: cardiac and self-report data

A description of statistical methods to analyze the cardiovascular and self-report data can be found in the Supplement. Briefly, linear mixed effects models were used to model the effects of time (baseline, stimulation, recovery), condition (sham, taVNS) and the time x condition interaction. Wilcoxon paired-samples tests were also used to compare differences in current intensity, pricking, pain, dull, and pressing sensations for sham and taVNS.

2.4. EEG preprocessing

EEG data were preprocessed using custom MATLAB scripts, EEGLAB [70], and Brainstorm [71]. The continuous raw EEG data were filtered between 1 Hz and 80 Hz using high-pass and low-pass finite impulse response filters, then down-sampled to 256 Hz. Cleanline was used to remove line, 25Hz stimulation artifact, and their harmonics. Artifact subspace reconstruction was used to remove bad data segments and reject noisy channels [72,73]. Omitted channels were interpolated using spherical spline. Data were re-referenced to the average (excluding bipolar channels), then EEG channels were submitted to independent components analysis (ICA) with data rank correction. Artifactual components were identified using the Multiple Artifact Rejection Algorithm (MARA) [74], a supervised machine learning algorithm. Posterior artifact probability >0.6 was used to mark components as artifactual. However, MARA did not successfully flag all residual stimulation artifacts. Therefore, the components for each EEG record were inspected. Those clearly reflecting stimulation artifact were manually removed.

2.5. Cardiovascular signal processing

For details on the processing of ECG and derivative cardiovascular variables, refer to the Supplement.

2.6. The heart evoked potential

Epoching. The R-R interval time series derived from the ECG data were used to generate event-marker files that were subsequently uploaded to the raw EEG time series and visually inspected for accuracy. Preprocessed EEG data were segmented from −200 ms to 700 ms relative to the peak of the R-wave. Baseline correction was applied from −200 ms to −50 ms.

Cardiac field artifact. To minimize the influence of the cardiac field artifact (CFA), which occurs due to volume conduction, the HEP epochs for scalp-level analyses were submitted to a Laplacian transformation using Brainstorm's Fieldtrip [75] plug-in. The Laplacian was not applied to the data submitted for source localization due to the assumptions required for computing current sources. See Supplement for further elaboration.

Sensor-level HEP statistical methodology. Baseline-corrected, then Laplacian transformed HEPs were averaged for each subject at each channel. To test for the two-tailed difference of taVNS − sham while controlling for the family-wise error rate, cluster-based permutation thresholding was applied on the spatiotemporal dimension from 175 to 500 ms [76,77]. See Supplement for details.

Current source reconstruction. Source modeling was carried out using the Brainstorm toolbox. EEG electrodes were co-registered using Nz, Iz, Cz, RPA and LPA as landmarks, then converting the coordinates to MNI space. The forward model was constructed with

the Open MEEG Boundary Element Method (BEM) [78] on the cortical surface using an MNI template brain, with a resolution of 45000 vertices. The inverse model was computed using constrained weighted minimum norm estimation (wMNE) with 2 mm FWHM smoothing, providing estimates of the magnitude of current activity at each vertex in units of Ampere-meters (A-m). Dynamical Statistical Parametric Mapping (dSPM) [79] was used to normalize the current estimates. For dSPM normalization, the full noise covariance matrix was computed from the baseline period defined from −200 to −50 ms. Default parameters were selected for depth weighting and noise regularization. Labels for cortical regions were defined according to the USCBrain Atlas [80].

3. Results

3.1. EEG

Sensor-level HEPs. Two clusters were found that exceeded the threshold for cluster-correction. The first cluster (cluster 1) reflected lower HEP voltage amplitudes for taVNS from 206 to 336 ms (Fig. 1). Cluster 1 was distributed primarily on the left frontocentral and centroparietal regions encompassing several electrodes (F7, FT7, FC5, T7, C5, CP5, TP7). On the right side, cluster 1 included FC6 and FT8. A second, right-lateralized cluster (cluster 2) was observed from 402 to 445 ms (Fig. 2), reflecting greater voltage amplitudes for taVNS, centered in centroparietal regions (CP4, CP6, TP8, P6, P8).

Source-level HEPs. To determine whether the sources of the sensor-level HEP differences could be reliably localized, two-tailed cluster-based permutation tests (n = 2000 permutations) were conducted using the Fieldtrip plug-in within the Brainstorm toolbox for the periods of time corresponding to the observed sensor-level cluster differences for taVNS - sham. Hence, two time periods were tested: 206 ms to 336 ms (cluster 1) and 402 ms to 445 ms (cluster 2). The periods were not averaged across time so that it would be possible to visualize the evolution of the HEP difference on the cortical surface within the timespan of the cluster.

Current sources of the HEP could be reliably identified for cluster 1 only; greater magnitude activity was observed for taVNS bilaterally in several lateral and medial sectors of the orbitofrontal cortex, anterior cingulate and subcallosal gyri. There was also a left-lateralized effect of taVNS, with greater magnitude activity originating from the operculum, postcentral gyrus, precentral gyrus, anterior and posterior insula, middle frontal gyrus (i.e., dorsolateral PFC), superior temporal gyrus, temporal pole, and anterior medial temporal regions. Source maps also indicated signal arising from non-cortical midline structures (Fig. 3a and b).

3.2. Heart Rate (HR) and Heart Rate Variability (HRV)

HR and HRV. No main effects of time, condition, or condition x time interaction effects were observed for any indices of HRV. However, a significant main effect of time was observed for HR, such that both taVNS and sham reduced HR during stimulation ($p = 0.035$). See Supplement for details.

3.3. Self-report

Further details are available in the Supplement. In brief:

STAI. Relative to baseline, state anxiety increased slightly, but consistently, during stimulation ($p = 0.000009$) and recovery ($p = 0.023$) regardless of stimulation condition.

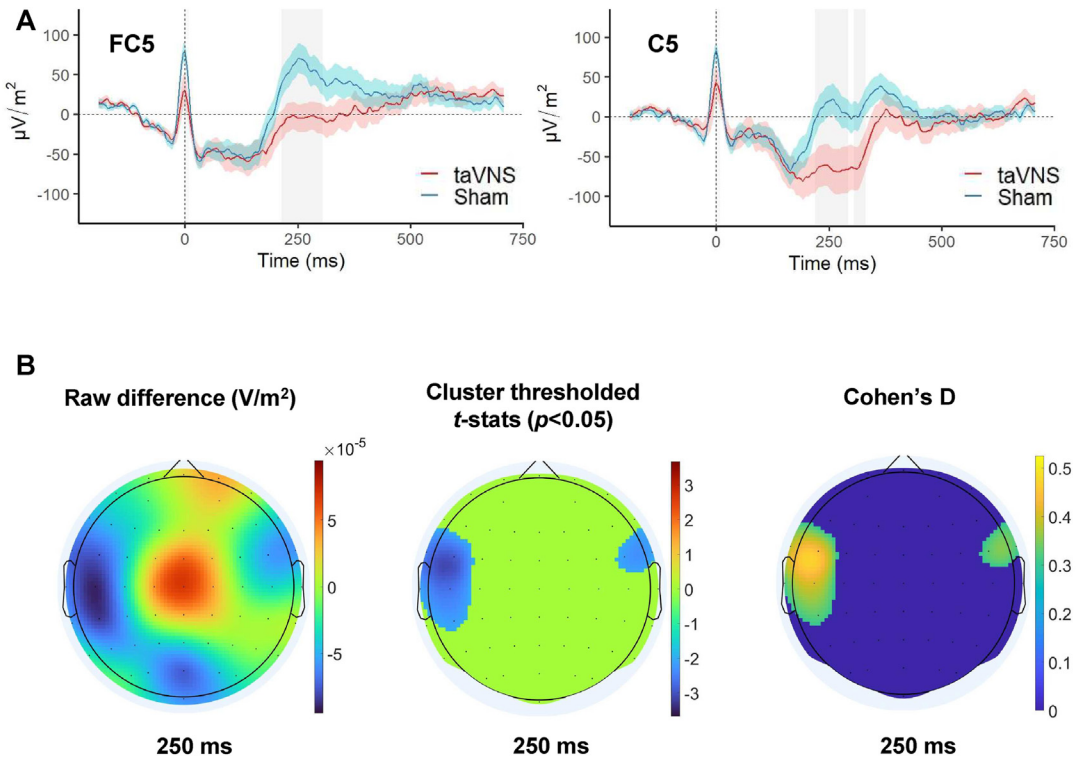

Fig. 1. Heart-evoked potential (HEP) analysis results for cluster 1. All differences were estimated using cluster-based permutation testing (cluster-threshold corrected $p < 0.05$, 2-tailed). **(A)** Two representative channels from cluster 1. Gray bars indicate significant time-points, shaded region represents the standard error of the mean. **(B)** HEP topography and statistics visualized at 250 ms. Left: raw voltage differences for taVNS − sham; middle: cluster thresholded statistics indicating significant locations of the HEP difference; right: conversion of HEP cluster-thresholded difference to an estimate of effect size.

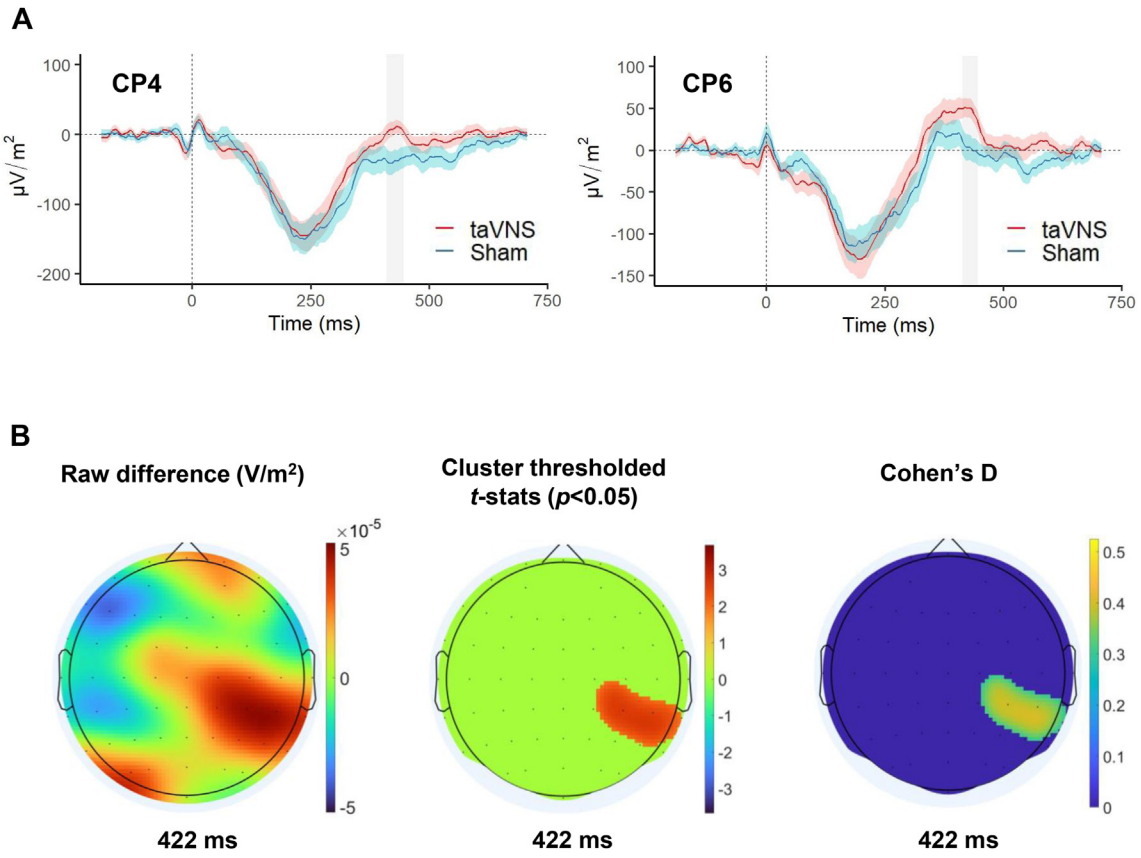

Fig. 2. Heart-evoked potential (HEP) analysis results for cluster 2. All differences were estimated using cluster-based permutation testing (cluster-threshold corrected $p < 0.05$, 2-tailed). **(A)** Two representative centroparietal channels. Gray bars indicate significant timepoints, shaded region represents the standard error of the mean. **(B)** HEP topography and statistics visualized at 422 ms. Left: raw voltage differences for taVNS − sham; middle: cluster thresholded statistics indicating significant locations of the HEP difference; right: conversion of HEP cluster-thresholded difference to an estimate of effect size.

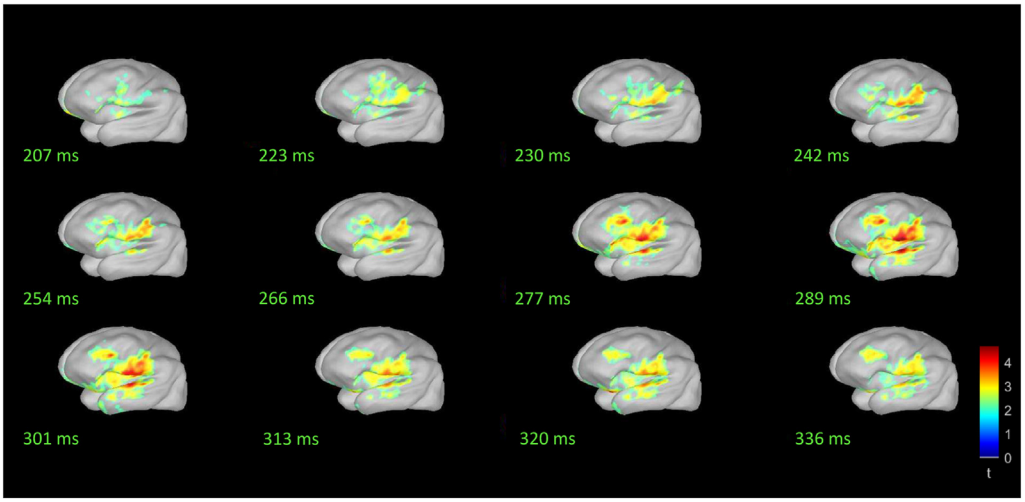

Fig. 3a. Estimated cortical current sources of the HEP cluster 1 (Fieldtrip cluster-based permutation testing, $p < 0.05$, 2-tailed), visualized on an inflated MNI template brain (left hemisphere). Contrast reflects the difference of taVNS − sham.

Current intensity and subjective stimulation qualities. Wilcoxon paired samples tests provided no evidence for differences in current intensity, pain, pricking, dull, or pressing sensations between sham and taVNS.

4. Discussion

We proposed that the interoceptive system may be accessed by taVNS. Accordingly, we investigated whether the HEP, an EEG-derived marker of cardiac interoceptive processing, could be

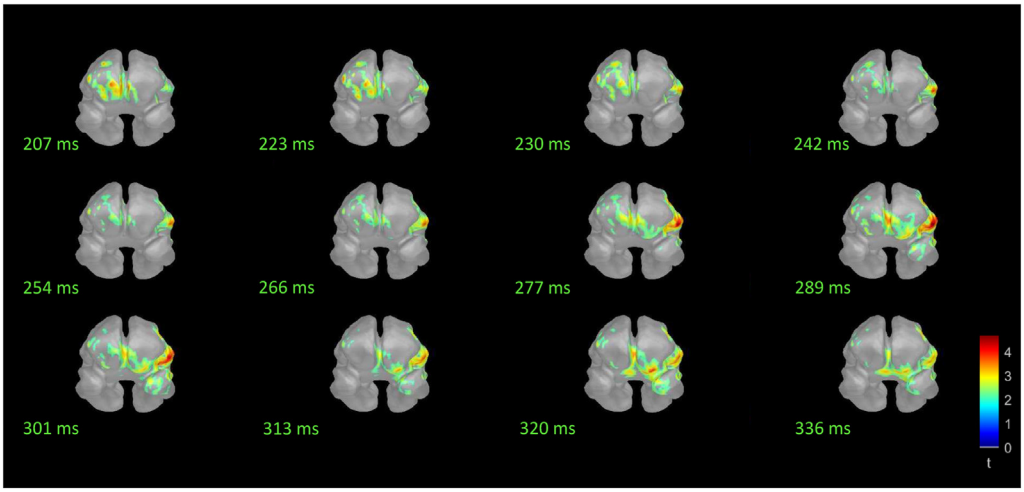

Fig. 3b. Estimated cortical current sources of the HEP cluster 1 (Fieldtrip cluster-based permutation testing, $p < 0.05$, 2-tailed), visualized on an inflated MNI template brain. Contrast reflects the difference of taVNS − sham. Visualized from a frontal-axial view.

modified by taVNS in healthy adult participants. Our first hypothesis was confirmed; taVNS modified HEP amplitudes at the scalp. Specifically, taVNS produced lower amplitude HEPs from 206 to 336 ms in left-lateralized central, centroparietal and frontotemporal electrodes and in bilateral frontocentral electrodes. taVNS also produced greater HEP amplitudes in right-lateralized centroparietal electrodes from 402 to 445 ms. We furthermore tested the hypothesis that taVNS modulation of HEPs would be associated with current sources that localize to the insula. Using BEM and wMNE we were able to identify the current sources of the cluster 1 HEP difference. Our second hypothesis of insula involvement was confirmed. However, the effect was localized not only to the (left) insula, but also to the left somatosensory cortex, operculum, middle frontal gyrus (corresponding to the dorsolateral PFC), as well as regions of the extended interoceptive-visceromotor network bilaterally, which included sectors of the OFC, subcallosal gyrus, and ACC.

To our knowledge, there is one prior report of HEP modulation by non-invasive VNS. Richter et al. (2020) used the GammaCore device (ElectroCore, LLC) to transcutaneously stimulate the cervical vagus nerve in a between-subjects design [81]. Substantial methodological differences make it difficult to directly compare the present results with Richter and colleagues' report. However, it should be considered that sham control in their study involved mild electrical stimulation that produces slight tingling sensations, whereas the active condition required strong currents that induce muscle contractions in the neck. Although they did not measure HEPs concurrent to stimulation, it is unclear whether their observations could have reflected off-target effects due to differences in current intensity rather than vagus nerve activation per se. For example, stimulation of muscle and cutaneous afferents are known to induce widespread cerebral, subcortical, and cerebellar responses [82]. Additionally, stronger physical sensations (e.g., muscle contractions in the face and neck) associated with active versus sham conditions during non-invasive brain stimulation acutely increase participant anxiety and may confound physiological responses of interest [83]. This is a relevant issue given that cortisol and arousal levels have been found to affect the HEP amplitude [52,84]. In the present study, we found that stimulation elicited a transient increase in participant anxiety, but that this effect did not depend on whether stimulation was active or sham. We also endeavored to match sensation qualities by using a method of limits and verified their similarity with self-report measures, thereby increasing confidence that the observed HEP effects do not reflect off-target sensory or cognitive-affective confounds.

The present study also provides an additional critical piece of evidence concerning the significance of the taVNS modulation of the HEP: confirmation of the involvement of the insula and functionally related regions. The patterns of localization we observed are consistent with prior MEG and EEG investigations, which have identified the operculum, anterior and posterior insula [53,56,85], somatosensory, cingulate, ventromedial prefrontal and orbitofrontal cortices [53,85–87] as sources of the HEP. Human intracranial EEG and ECoG studies have likewise recorded HEPs from the insula, operculum, cingulate, amygdala, medial temporal lobes, somatosensory cortex, orbitofrontal cortex, and inferior frontal gyrus [50,62–64]. Notably, Park et al. (2017) recorded intracranial EEG yielding 474 bipolar derivations from multiple cortical and subcortical regions; significant HEP activity was concentrated primarily in the insula and operculum with voltage deflections occurring from approximately 200–400 ms [62]. This is a spatiotemporal feature that may parallel the cluster 1 HEP effect observed in the present study.

We observed strong left-lateralization of HEP current sources for the difference of taVNS – sham, an effect not anticipated in our hypotheses. Tentatively, a lateralized response may reflect the organization of ascending pathways from the NST. Specifically, L1 inputs are represented contralaterally in the cortex, whereas NST afferents may ascend to the cortex ipsilaterally or bilaterally, although the current understanding of this issue is incomplete [6,7,88–90]. However, activation of the NST ipsilateral to the side of stimulation is commonly observed in fMRI studies using taVNS [35,36,38,43], including greater functional connectivity between the left NST and the left anterior insula and left anterior/midcingulate cortex [35]. Enhanced insula metabolism ipsilateral to the side of stimulation has also been reported as a (ta)VNS treatment outcome for patients with depression [90,91]. Lateralized modulation of interoceptive pathways by (ta)VNS, and its clinical impact on disorders of stress and distress may bear upon the hypothesis of forebrain emotional asymmetry, which proposes that the lateralization of emotion processing in the brain arises from the asymmetrical organization of autonomic nervous system peripherally and within brainstem autonomic sites [88,92].

The underlying neural and physiological generative mechanisms of HEPs have not been firmly established. However, HEPs are believed to reflect beat-to-beat cardiovascular dynamics that are

transduced via the baroreceptors (mediated by the vagus and glossopharyngeal nerves), intrinsic cardiac neurons (vagal and spinothalamic L1 pathways), and cutaneous mechanoreceptors (medial lemniscal pathway) [50]. Each of these elements may contribute to different components of the HEP waveform, potentially at varying latencies, although the correspondence of HEP components to specific cardiovascular parameters remains an open question. Consequently, the precise neural inputs responsible for the present findings remain to be elucidated. It should be considered that taVNS likely modulates the activity of multiple interacting cranial nerve pathways and thereby, sources of interoceptive inputs to the cortex [40]. In other words, the neural effects of taVNS are unlikely to be *purely* mediated by direct vagus nerve modulation of the NST [40]. Therefore, HEP modulation by taVNS may be best understood as a broad measure of functional integration within the interoceptive network.

The interoceptive system has already demonstrated predictive value for VNS treatment outcomes in drug-resistant epilepsy. Machine learning algorithms were trained to predict anticonvulsant response to chronic VNS based on presurgical levels of resting-state functional connectivity of the thalamus with the ACC and left insula [93]. Using an out-of-sample test cohort, the trained model could predict VNS anticonvulsant efficacy with 88% accuracy [93]. Our own group has reported that in patients with epilepsy, VNS responders versus non-responders exhibited greater source current activity in the insula, OFC, and limbic system when their devices were turned on [94], and that anticonvulsant response to chronic VNS was positively associated patients' presurgical levels of parasympathetically-mediated HRV [95].

HEPs may hold promise as a biomarker in taVNS clinical neuroscience trials. However, the steps to validation are substantial. Beyond identifying neuroimaging features that reflect biologically meaningful mechanisms, standardized procedures must be defined for extracting features. Moreover, the sensitivity, specificity, and generalizability of these features (i.e., via cross-validation) [96] must be established for a given population. The current study offers initial insights into the possible utility of the HEP to the degree that it reflects functional properties of the interoceptive system that is modifiable by taVNS, and to the degree that such modification reduces symptom burdens in patient populations indicated for taVNS.

We performed permutation analyses using all EEG sensors within the relevant window of time [62] to facilitate source analyses in a hypothesis-driven, but unbiased manner. The cluster 1 results were highly convergent with peak spatiotemporal effects identified meta-analytically [52]. The results provide an initial search space for HEP feature extraction in biomarker validation studies. While summary features from HEPs could be defined in many ways, we suggest that for a study seeking to establish, for example, the predictive value of the HEP in prospective taVNS trials, it may be useful to average patients' differential HEP curves within source-localized or sensor-based regions-of-interest to active taVNS versus sham prior to treatment within time-windows informed either by the present study or by meta-analysis [52].

4.1. Limitations

We applied sophisticated methods to estimate the forward and inverse solution, yet the head and brain models could not be optimized to the individual with an unknown effect on the spatial precision of the estimates. An optimized source reconstruction scheme could be achieved by obtaining each subject's MRI, in combination with high-density EEG and 3D scanners to precisely co-register the sensors to locations on the scalp [97,98]. Additionally, contamination from the CFA is a primary concern for HEPs recorded from the scalp as there are no perfect solutions for removal. However, we found no differences in ECG morphology (see Supplemental Fig. S1), indicating that it is an unlikely explanation for the HEP results. We further applied a Laplacian transformation to reduce the impact of the CFA. These steps, along with evidence that the current sources of the HEP effect correspond to current understanding of NST/L1 cortical projections, increase confidence that the present findings do not reflect artifacts.

Although our hypotheses were confirmed, a challenge shared with many taVNS studies is the choice of sham control. The earlobe is innervated by the GAN, a branch of the spinal cervical plexus with origins in C2 and C3 whose fibers terminate in the nucleus cuneatus and spinal trigeminal nucleus [99]. Crosstalk among spinal and cranial nerves, collateral projections from the spinal trigeminal nucleus to the NST and trigeminal-autonomic reflexes are also well-characterized [40,100]. Consequently, earlobe stimulation provides a conservative control condition that may reach brainstem targets that overlap with those of the AVBN [101,102]. For instance, both sham and taVNS elicited heart rate reductions in our study. However, a conservative control may be advantageous if subtracting out its effect reflects greater specificity of the AVBN's vagal influence on brain activity. Lastly, we used a specific set of stimulation parameters consistent with the CE-marking of the device used (with a modified duty-cycle pre-programmed for us by the manufacturers for investigational purposes). Future studies should examine the parameter-dependence of taVNS modulation of HEPs. It should also be considered that our effect was observed in healthy adults during acute stimulation; the persistence of a taVNS effect on the HEP remains to be demonstrated in clinical populations.

5. Conclusion

HEPs are sensitive to acute stimulation of the AVBN via the left cymba conchae and the effect arises from a cortical network involved in interoception. Although methodological choices need to be carefully considered when performing HEP analyses, and a consensus would enhance comparability across studies [50,52], the confirmation that taVNS modulates interoceptive neural processing indicates the possible relevance of this system to taVNS mechanism of action. Neural activity associated with the interoceptive pathway as indexed by HEPs may therefore serve as an objective, non-invasive outcome parameter for the cortical effects of taVNS. While many steps to validation remain before the HEP may be considered a potential biomarker in clinical neuroscience investigations, the current study provides a starting point for discovery.

Funding

This study was supported by a Graduate Research Fellowship from the National Science Foundation (DGE-1418060) and a Belgian American Educational Foundation (BAEF) fellowship to TP. KV and MAV are funded by special research grants from Ghent University. KV is also funded by a grant from Het Fonds Wetenschappelijk Onderzoek – Vlaanderen (FWO) (WOG-tVNS group). EC is funded by a Geneeskundige Stichting Koningin Elisabeth (GSKE) fellowship. The funders had no influence on the study design; in the collection, analysis, or interpretation of data; in the writing of the report; or the decision to submit the article for publication.

Declaration of competing interest

KV received free devices from Cerbomed for research studies in healthy adult volunteers, which includes this study. KV has also received consultancy fees from and participated in advisory board

meeting for LivaNova, Synergia Medical and the Alfred E. Mann Foundation.

Data statement

The datasets generated during and/or analyzed during the current study are available from the corresponding author upon reasonable request. Preprocessing and analysis scripts are publicly available at: https://github.com/taVNS-HEP-study/Scripts.

CRediT authorship contribution statement

Tasha Poppa: Conceptualization, Funding acquisition, Project administration, Investigation, Formal analysis, Programming, Visualization, Writing – original draft, Writing – review & editing. **Lars Benschop:** Programming, Formal analysis, Visualization, Writing – review & editing. **Paula Horczak:** Investigation, Project administration, Writing – review & editing. **Marie-Anne Vanderhasselt:** Supervision, Project administration, Writing – review & editing. **Evelien Carrette:** Resources, Writing – review & editing. **Antoine Bechara:** Supervision, Project administration, Writing – review & editing. **Chris Baeken:** Supervision, Writing – review & editing. **Kristl Vonck:** Resources, Supervision, Writing – review & editing.

Acknowledgements

We are thankful to Daniele Marinazzo for his helpful comments during the drafting of this manuscript.

Appendix A. Supplementary data

Supplementary data to this article can be found online at https://doi.org/10.1016/j.brs.2021.12.004.

References

[1] Burger AM, D'Agostini M, Verkuil B, van Diest I. Moving beyond belief: a narrative review of potential biomarkers for transcutaneous vagus nerve stimulation. Psychophysiology 2020;57(6):e13571. https://doi.org/10.1111/psyp.13571.
[2] Craig AD. How do you feel? Interoception: the sense of the physiological condition of the body. Nat Rev Neurosci 2002;3:655–66.
[3] Khalsa SS, et al. "Interoception and mental health: a roadmap. Biol Psychiatr: Cognitive Neurosci Neuroimag 2018;3(6):501–13. https://doi.org/10.1016/j.bpsc.2017.12.004.
[4] Beggs J, Jordan S, Ericson A-C, Blomqvist A, Craig AD. Synaptology of trigemino- and spinothalamic lamina I terminations in the posterior ventral medial nucleus of the macaque. J Comp Neurol 2003;459:334–54. https://doi.org/10.1002/cne.10613.
[5] Feldman Barrett L, Simmons WK. Interoceptive predictions in the brain. Nat Rev Neurosci 2015;16(7):419–29. https://doi.org/10.1038/nrn3950.
[6] Evrard HC. The organization of the primate insular cortex. Front Neuroanat 2019;13:43. https://doi.org/10.3389/fnana.2019.00043.
[7] Palma J-A, Benarroch EE. Neural control of the heart. Neurology 2014;83(3):261–71. https://doi.org/10.1212/WNL.0000000000000605.
[8] Michopoulos V, Vester A, Neigh G. Posttraumatic stress disorder: a metabolic disorder in disguise? Exp Neurol 2016;284:220–9. https://doi.org/10.1016/j.expneurol.2016.05.038.
[9] Michopoulos V, Powers A, Gillespie CF, Ressler KJ, Jovanovic T. Inflammation in fear- and anxiety-based disorders: PTSD, GAD, and beyond. Neuropsychopharmacology 2017;42(1):254–70. https://doi.org/10.1038/npp.2016.146.
[10] Savitz J, Harrison NA. Interoception and inflammation in psychiatric disorders. Biol Psychiatr: Cognitive Neurosci Neuroimag 2018;3(6):514–24. https://doi.org/10.1016/j.bpsc.2017.12.011.
[11] Beauchaine TP. Respiratory sinus arrhythmia: a transdiagnostic biomarker of emotion dysregulation and psychopathology. Curr Opinion Psychol 2015;3:43–7. https://doi.org/10.1016/j.copsyc.2015.01.017.
[12] Koch C, Wilhelm M, Salzmann S, Rief W, Euteneuer F. A meta-analysis of heart rate variability in major depression. Psychol Med 2019;49(12):1948–57. https://doi.org/10.1017/S0033291719001351.
[13] Iob E, Kirschbaum C, Steptoe A. Persistent depressive symptoms, HPA-axis hyperactivity, and inflammation: the role of cognitive-affective and somatic symptoms. Mol Psychiatr 2020;25(5):1130–40. https://doi.org/10.1038/s41380-019-0501-6.
[14] Knaster P, Karlsson H, Estlander A-M, Kalso E. Psychiatric disorders as assessed with SCID in chronic pain patients: the anxiety disorders precede the onset of pain. Gen Hosp Psychiatr 2012;34(1):46–52. https://doi.org/10.1016/j.genhosppsych.2011.09.004.
[15] Velly AM, Mohit S. Epidemiology of pain and relation to psychiatric disorders. Prog Neuro Psychopharmacol Biol Psychiatr 2018;87:159–67. https://doi.org/10.1016/j.pnpbp.2017.05.012.
[16] Milaneschi Y, Simmons WK, van Rossum EFC, Penninx BW. Depression and obesity: evidence of shared biological mechanisms. Mol Psychiatr Jan. 2019;24(1). https://doi.org/10.1038/s41380-018-0017-5.
[17] Lydecker JA, Grilo CM. Psychiatric comorbidity as predictor and moderator of binge-eating disorder treatment outcomes: an analysis of aggregated randomized controlled trials. Psychol Med 2021:1–9. https://doi.org/10.1017/S0033291721001045.
[18] Gianaros PJ, Sheu LK. A review of neuroimaging studies of stressor-evoked blood pressure reactivity: emerging evidence for a brain-body pathway to coronary heart disease risk. Neuroimage 2009;47(3):922–36. https://doi.org/10.1016/j.neuroimage.2009.04.073.
[19] Kraynak TE, Marsland AL, Gianaros PJ. Neural mechanisms linking emotion with cardiovascular disease. Curr Cardiol Rep 2018;20(12):128. https://doi.org/10.1007/s11886-018-1071-y.
[20] Ginty AT, Kraynak TE, Fisher JP, Gianaros PJ. Cardiovascular and autonomic reactivity to psychological stress: neurophysiological substrates and links to cardiovascular disease. Auton Neurosci 2017;207:2–9. https://doi.org/10.1016/j.autneu.2017.03.003.
[21] Wu H, et al. Covariation between spontaneous neural activity in the insula and affective temperaments is related to sleep disturbance in individuals with major depressive disorder. Psychol Med 2021;51(5):731–40. https://doi.org/10.1017/S0033291719003647.
[22] Li H, et al. Altered heartbeat perception sensitivity associated with brain structural alterations in generalised anxiety disorder. Gen Psychiatr Feb. 2020;33(1). https://doi.org/10.1136/gpsych-2019-100057. e100057–e100057.
[23] Gray JP, Müller VI, Eickhoff SB, Fox PT. Multimodal abnormalities of brain structure and function in major depressive disorder: a meta-Analysis of neuroimaging studies. Am J Psychiatr 2020;177(5):422–34. https://doi.org/10.1176/appi.ajp.2019.19050560.
[24] Dalton KM, Kalin NH, Grist TM, Davidson RJ. Neural-cardiac coupling in threat-evoked anxiety. J Cognit Neurosci Jun. 2005;17(6):969–80. https://doi.org/10.1162/0898929054021094.
[25] Schmaal L, et al. Enigma MDD: seven years of global neuroimaging studies of major depression through worldwide data sharing. Transl Psychiatry 2020;10(1):172. https://doi.org/10.1038/s41398-020-0842-6.
[26] Baeken C, et al. Accelerated HF-rTMS in treatment-resistant unipolar depression: insights from subgenual anterior cingulate functional connectivity. World J Biol Psychiatr 2014;15(4):286–97. https://doi.org/10.3109/15622975.2013.872295.
[27] Thome J, et al. Desynchronization of autonomic response and central autonomic network connectivity in posttraumatic stress disorder. Hum Brain Mapp 2016;38(1):27–40. https://doi.org/10.1002/hbm.23340. Sep.
[28] Goodkind M, et al. Identification of a common neurobiological substrate for mental illness. JAMA Psychiatr Apr. 2015;72(no. 4). https://doi.org/10.1001/jamapsychiatry.2014.2206.
[29] Goessl VC, Curtiss JE, Hofmann SG. The effect of heart rate variability biofeedback training on stress and anxiety: a meta-analysis. 2017. p. 2578–86. https://doi.org/10.1017/S0033291717001003.
[30] Lehrer P, et al. Heart rate variability biofeedback improves emotional and physical health and performance: a systematic review and meta-analysis. Appl Psychophysiol Biofeedback 2020;45(3):109–29. https://doi.org/10.1007/s10484-020-09466-z.
[31] Gurel NZ, et al. Transcutaneous cervical vagal nerve stimulation reduces sympathetic responses to stress in posttraumatic stress disorder: a double-blind, randomized, sham controlled trial. Neurobiol Stress 2020;13:100264. https://doi.org/10.1016/j.ynstr.2020.100264.
[32] Lamb DG, Porges EC, Lewis GF, Williamson JB. Non-invasive vagal nerve stimulation effects on hyperarousal and autonomic state in patients with posttraumatic stress disorder and history of mild traumatic brain injury: preliminary evidence. Front Med 2017;4:124. https://doi.org/10.3389/fmed.2017.00124.
[33] Weng HY, Feldman JL, Leggio L, Napadow V, Park J, Price CJ. Interventions and manipulations of interoception. Trends Neurosci 2021;44(1):52–62. https://doi.org/10.1016/j.tins.2020.09.010.
[34] Thrivikraman Kv, Zejnelovic F, Bonsall RW, Owens MJ. Neuroendocrine homeostasis after vagus nerve stimulation in rats. Psychoneuroendocrinology 2013;38(7):1067–77. https://doi.org/10.1016/j.psyneuen.2012.10.015.
[35] Garcia RG, Lin RL, Lee J, Kim J, Barbieri R, Sclocco R. Modulation of brainstem activity and connectivity by respiratory-gated auricular vagal afferent nerve stimulation in migraine patients. Pain 2017;158(8):1461–72. https://doi.org/10.1097/j.pain.0000000000000930.
[36] Frangos E, Ellrich J, Komisaruk BR. Non-invasive access to the vagus nerve central projections via electrical stimulation of the external ear: fMRI

evidence in humans. Brain Stimul 2015;8(3):624–36. https://doi.org/10.1016/j.brs.2014.11.018.
[37] Yakunina N, Kim SS, Nam E-C. Optimization of transcutaneous vagus nerve stimulation using functional MRI. Neuromodulation 2017;20:290–300. https://doi.org/10.1111/ner.12541.
[38] Sclocco R, et al. Stimulus frequency modulates brainstem response to respiratory-gated transcutaneous auricular vagus nerve stimulation. Brain Stimul 2020;13(4):970–8. https://doi.org/10.1016/j.brs.2020.03.011.
[39] Zhang Y, et al. Transcutaneous auricular vagus nerve stimulation at 1 Hz modulates locus coeruleus activity and resting state functional connectivity in patients with migraine: an fMRI study. Neuroimage: Clinical 2019;24:101971. https://doi.org/10.1016/j.nicl.2019.101971.
[40] Cakmak YO. Concerning auricular vagal nerve stimulation: occult neural networks. Front Hum Neurosci 2019;13:421. https://doi.org/10.3389/fnhum.2019.00421.
[41] Butt MF, Albusoda A, Farmer AD, Aziz Q. The anatomical basis for transcutaneous auricular vagus nerve stimulation. J Anat Apr. 2020;236(4). https://doi.org/10.1111/joa.13122.
[42] Ay I, Napadow V, Ay H. Electrical stimulation of the vagus nerve dermatome in the external ear is protective in rat cerebral ischemia. Brain Stimul Jan. 2015;8(1):7–12. https://doi.org/10.1016/j.brs.2014.09.009.
[43] Sclocco R, et al. The influence of respiration on brainstem and cardiovagal response to auricular vagus nerve stimulation: a multimodal ultrahigh-field (7T) fMRI study. Brain Stimul 2019;12(4):911–21. https://doi.org/10.1016/j.brs.2019.02.003.
[44] Dietrich S, et al. A novel transcutaneous vagus nerve stimulation leads to brainstem and cerebral activations measured by functional MRI. Biomed Tech 2008;53(3):104–11. https://doi.org/10.1515/BMT.2008.022.
[45] Zhang Y, et al. Transcutaneous auricular vagus nerve stimulation at 1 Hz modulates locus coeruleus activity and resting state functional connectivity in patients with migraine: an fMRI study. Neuroimage: Clinical 2019;24:101971. https://doi.org/10.1016/j.nicl.2019.101971.
[46] Ruffoli R, Giorgi FS, Pizzanelli C, Murri L, Paparelli A, Fornai F. The chemical neuroanatomy of vagus nerve stimulation. J Chem Neuroanat 2011;42(4):288–96. https://doi.org/10.1016/j.jchemneu.2010.12.002.
[47] Badran BW, et al. Neurophysiologic effects of transcutaneous auricular vagus nerve stimulation (taVNS) via electrical stimulation of the tragus: a concurrent taVNS/fMRI study and review. Brain Stimul May 2018;11(3):492–500. https://doi.org/10.1016/j.brs.2017.12.009.
[48] Kraus T, Kiess O, Hösl K, Terekhin P, Kornhuber J, Forster C. CNS BOLD fMRI effects of sham-controlled transcutaneous electrical nerve stimulation in the left outer auditory canal – a pilot study. Brain Stimul 2013;6(5):798–804. https://doi.org/10.1016/j.brs.2013.01.011.
[49] Zhang Y, et al. Transcutaneous auricular vagus nerve stimulation (taVNS) for migraine: an fMRI study. Reg Anesthesia Pain Med Feb. 2021;46(2):145. https://doi.org/10.1136/rapm-2020-102088.
[50] Park H-D, Blanke O. Heartbeat-evoked cortical responses: underlying mechanisms, functional roles, and methodological considerations. Neuroimage 2019;197:502–11. https://doi.org/10.1016/j.neuroimage.2019.04.081.
[51] Schandry R, Montoya P. Event-related brain potentials and the processing of cardiac activity. Biol Psychol 1996;42:75–85. https://doi.org/10.1016/0301-0511(95)05147-3.
[52] Coll M-P, Hobson H, Bird G, Murphy J. Systematic review and meta-analysis of the relationship between the heartbeat-evoked potential and interoception. Neurosci Biobehav Rev 2021;122:190–200. https://doi.org/10.1016/j.neubiorev.2020.12.012.
[53] Pollatos O, Kirsch W, Schandry R. Brain structures involved in interoceptive awareness and cardioafferent signal processing: a dipole source localization study. Hum Brain Mapp 2005;64:54–64. https://doi.org/10.1002/hbm.20121.
[54] Pollatos O, Schandry R. Accuracy of heartbeat perception is reflected in the amplitude of the heartbeat-evoked brain potential. Psychophysiology 2004;41:476–82. https://doi.org/10.1111/1469-8986.2004.00170.x.
[55] Gentsch A, Sel A, Marshall AC, Schütz-Bosbach S. Affective interoceptive inference: evidence from heart-beat evoked brain potentials. Hum Brain Mapp 2019;40(1):20–33. https://doi.org/10.1002/hbm.24352.
[56] Couto B, et al. Heart evoked potential triggers brain responses to natural affective scenes: a preliminary study. Auton Neurosci 2015;193:132–7. https://doi.org/10.1016/j.autneu.2015.06.006.
[57] Terhaar J, Viola FC, Bär K-J, Debener S. Heartbeat evoked potentials mirror altered body perception in depressed patients. Clin Neurophysiol 2012;123(10):1950–7. https://doi.org/10.1016/j.clinph.2012.02.086.
[58] Pang J, et al. Altered interoceptive processing in generalized anxiety disorder—a heartbeat-evoked potential research. Front Psychiatr 2019;10:616. Available, https://www.frontiersin.org/article/10.3389/fpsyt.2019.00616.
[59] Yoris A, et al. Multilevel convergence of interoceptive impairments in hypertension: new evidence of disrupted body-brain interactions. Hum Brain Mapp 2018;39(4):1563–81. https://doi.org/10.1002/hbm.23933. Apr.
[60] Gray MA, et al. A cortical potential reflecting cardiac function. Proc Natl Acad Sci USA 2007;104(16):6818–23. https://doi.org/10.1073/pnas.0609509104.
[61] Leopold C, Schandry R. The heartbeat-evoked brain potential in patients suffering from diabetic neuropathy and in healthy control persons 2001;112:674–82.
[62] Park H, et al. Neural sources and underlying mechanisms of neural responses to heartbeats, and their role in bodily self-consciousness: an intracranial EEG study. Cerebr Cortex 2017:1–14. https://doi.org/10.1093/cercor/bhx136.
[63] Kern M, Aertsen A, Schulze-Bonhage A, Ball T. Heart cycle-related effects on event-related potentials, spectral power changes, and connectivity patterns in the human ECoG. Neuroimage 2013;81:178–90. https://doi.org/10.1016/j.neuroimage.2013.05.042.
[64] Canales-Johnson A, et al. Auditory feedback differentially modulates behavioral and neural markers of objective and subjective performance when tapping to your heartbeat. Cerebr Cortex Nov. 2015;25(11):4490–503. https://doi.org/10.1093/cercor/bhv076.
[65] Spielberger CD. Manual for the state-trait anxiety inventory. Palo Alto, CA: Consulting Psychologists Press; 1983.
[66] Beissner F, et al. Quick discrimination of Adelta and C Fiber mediated pain based on three verbal descriptors. PLoS One Sep. 2010;5(9). https://doi.org/10.1371/journal.pone.0012944.
[67] Farmer AD, et al. International consensus based review and recommendations for minimum reporting standards in research on transcutaneous vagus nerve stimulation (version 2020). Front Hum Neurosci 2021;14:409. https://doi.org/10.3389/fnhum.2020.568051.
[68] Larsen LE, et al. Vagus nerve stimulation applied with a rapid cycle has more profound influence on hippocampal electrophysiology than a standard cycle. Neurotherapeutics 2016:592–602. https://doi.org/10.1007/s13311-016-0432-8.
[69] Ellrich J. Transcutaneous vagus nerve stimulation. Eur Neurol Rev 2011;6(4):2–4. https://doi.org/10.17925/ENR.2011.06.04.254.
[70] Delorme A, Makeig S. EEGLAB: an open source toolbox for analysis of single-trial EEG dynamics including independent component analysis. J Neurosci Methods 2004;134:9–21. https://doi.org/10.1016/j.jneumeth.2003.10.009.
[71] Tadel F, Baillet S, Mosher JC, Pantazis D, Leahy RM. Brainstorm: a user-friendly application for MEG/EEG analysis. Comput Intell Neurosci 2011:879716. https://doi.org/10.1155/2011/879716. 2011.
[72] Kothe CA, Makeig S. "BCILAB: a platform for brain–computer interface development. J Neural Eng 2013;10(5). https://doi.org/10.1088/1741-2560/10/5/056014. 056014.
[73] Chang C-Y, Hsu S-H, Pion-Tonachini L, Jung T-P. Evaluation of artifact subspace reconstruction for automatic EEG artifact removal 2018;2018. https://doi.org/10.1109/EMBC.2018.8512547.
[74] Winkler I, Brandl S, Horn F, Waldburger E, Allefeld C, Tangermann M. Robust artifactual independent component classification for BCI practitioners. J Neural Eng May 2014;11(3):35013. https://doi.org/10.1088/1741-2560/11/3/035013.
[75] Oostenveld R, Fries P, Maris E, Schoffelen J-M. FieldTrip: open source software for advanced analysis of MEG, EEG, and invasive electrophysiological data,. Comput Intell Neurosci 2011;2011:156869. https://doi.org/10.1155/2011/156869.
[76] Maris E, Oostenveld R. Nonparametric statistical testing of EEG- and MEG-data. J Neurosci Methods 2007;164(1):177–90. https://doi.org/10.1016/j.jneumeth.2007.03.024.
[77] Benschop L, Baeken C, Vanderhasselt M-A, van de Steen F, van Heeringen K, Arns M. "Electroencephalogram resting state frequency power characteristics of suicidal behavior in female patients with major depressive disorder. J Clin Psychiatr Oct. 2019;80(6). https://doi.org/10.4088/JCP.18m12661.
[78] Gramfort A, Papadopoulo T, Olivi E, Clerc M. "OpenMEEG: opensource software for quasistatic bioelectromagnetics. Biomed Eng Online Sep. 2010;9(1):45. https://doi.org/10.1186/1475-925X-9-45.
[79] Dale AM, et al. Dynamic statistical parametric mapping: combining fMRI and MEG for high-resolution imaging of cortical activity. Neuron 2000;26(1):55–67. https://doi.org/10.1016/S0896-6273(00)81138-1.
[80] Joshi AA, et al. A hybrid high-resolution anatomical MRI atlas with sub-parcellation of cortical gyri using resting fMRI. bioRxiv 2020. https://doi.org/10.1101/2020.09.12.294322.
[81] Richter F, et al. Behavioral and neurophysiological signatures of interoceptive enhancements following vagus nerve stimulation. Hum Brain Mapp Apr. 2021;42(no. 5). https://doi.org/10.1002/hbm.25288.
[82] Wardman DL, Gandevia SC, Colebatch JG. Cerebral, subcortical, and cerebellar activation evoked by selective stimulation of muscle and cutaneous afferents: an fMRI study. Physiol Rep Apr. 2014;2(no. 4). https://doi.org/10.1002/phy2.270.
[83] Poppa T, de Witte S, Vanderhasselt M-A, Bechara A, Baeken C. Theta-burst stimulation and frontotemporal regulation of cardiovascular autonomic outputs: the role of state anxiety. Int J Psychophysiol 2020;149. https://doi.org/10.1016/j.ijpsycho.2019.12.011.
[84] Schulz A, Strelzyk F, Ferreira de Sá DS, Naumann E, Vögele C, Schächinger H. Cortisol rapidly affects amplitudes of heartbeat-evoked brain potentials—implications for the contribution of stress to an altered perception of physical sensations? Psychoneuroendocrinology 2013;38(11):2686–93. https://doi.org/10.1016/j.psyneuen.2013.06.027.
[85] Babo-Rebelo M, Richter CG, Tallon-Baudry C. Neural responses to heartbeats in the default network encode the self in spontaneous thoughts. J Neurosci 2016;36(30):7829–40. https://doi.org/10.1523/JNEUROSCI.0262-16.2016.
[86] Park H, Correia S, Ducorps A, Tallon-baudry C. Spontaneous fluctuations in neural responses to heartbeats predict visual detection 2014;17(4). https://doi.org/10.1038/nn.3671.

[87] Jiang H, et al. "Brain–heart interactions underlying traditional Tibetan Buddhist meditation,". Cerebr Cortex 2019. https://doi.org/10.1093/cercor/bhz095. Jun.
[88] Craig A D (Bud). Forebrain emotional asymmetry: a neuroanatomical basis? Trends Cognit Sci 2005;9(12):566–71. https://doi.org/10.1016/j.tics.2005.10.005.
[89] Beckstead RM, Morse JR, Norgren R. The nucleus of the solitary Tract in the monkey: projections to the thalamus and brain stem nuclei. J Comp Neurol 1980;190(2):259–82. https://doi.org/10.1002/cne.901900205.
[90] Pritchard TC, Macaluso DA, Eslinger PJ. Taste perception in patients with insular cortex lesions. Behav Neurosci 1999;113(4). https://doi.org/10.1037/0735-7044.113.4.663.
[91] Kosel M, Brockmann H, Frick C, Zobel A, Schlaepfer TE. Chronic vagus nerve stimulation for treatment-resistant depression increases regional cerebral blood flow in the dorsolateral prefrontal cortex. Psychiatr Res Neuroimaging Mar. 2011;191(3):153–9. https://doi.org/10.1016/j.pscychresns.2010.11.004.
[92] Strigo IA, Craig AD (Bud). Interoception, homeostatic emotions and sympathovagal balance. Philos Trans R Soc Lond B Biol Sci 2016;371(1708). https://doi.org/10.1098/rstb.2016.0010.
[93] Ibrahim GM, et al. Presurgical thalamocortical connectivity is associated with response to vagus nerve stimulation in children with intractable epilepsy. Neuroimage: Clinical 2017;16:634–42. https://doi.org/10.1016/j.nicl.2017.09.015.
[94] Wostyn S, et al. EEG derived brain activity reflects treatment response from vagus nerve stimulation in patients with epilepsy. Int J Neural Syst 2016;27:1650048. https://doi.org/10.1142/S0129065716500489. 04.
[95] Hödl S, et al. Neurophysiological investigations of drug resistant epilepsy patients treated with vagus nerve stimulation to differentiate responders from non-responders. Eur J Neurol Jul. 2020;27(7):1178–89. https://doi.org/10.1111/ene.14270.
[96] van der Miesen MM, Lindquist MA, Wager TD. Neuroimaging-based biomarkers for pain: state of the field and current directions. PAIN Rep 2019;4(e751). https://doi.org/10.1097/PR9.0000000000000751.
[97] Koessler L, et al. Automated cortical projection of EEG sensors: anatomical correlation via the international 10 − 10 system. Neuroimage 2009;46(1):64–72. https://doi.org/10.1016/j.neuroimage.2009.02.006.
[98] Taberna GA, Marino M, Ganzetti M, Mantini D. Spatial localization of EEG electrodes using 3D scanning. J Neural Eng Apr. 2019;16(2). https://doi.org/10.1088/1741-2552/aafdd1.
[99] Liu D, Hu Y. The central projections of the great auricular nerve primary afferent fibers — an HRP transganglionic tracing method. Brain Res Apr. 1988;445(2). https://doi.org/10.1016/0006-8993(88)91179-1.
[100] Möller M, Mehnert J, May A. Hypothalamic activation discriminates painful and non-painful initiation of the trigeminal autonomic reflex - an fMRI study. Cephalalgia 2020;40(1):79–87. https://doi.org/10.1177/0333102419868191.
[101] Keute M, Ruhnau P, Zaehle T. Reply to 'Reconsidering sham in transcutaneous vagus nerve stimulation studies. Clin Neurophysiol Nov. 2018;129(11). https://doi.org/10.1016/j.clinph.2018.09.001.
[102] Rangon C-M. Reconsidering sham in Transcutaneous vagus nerve stimulation studies. Clin Neurophysiol Nov. 2018;129(11). https://doi.org/10.1016/j.clinph.2018.08.027.